



**HAL**  
open science

# Future Drought-Induced Tree Mortality Risk in Amazon Rainforest

Yitong Yao, Philippe Ciais, Emilie Joetzjer, Songbai Hong, Wei Li, Lei Zhu,  
Nicolas Viovy

► **To cite this version:**

Yitong Yao, Philippe Ciais, Emilie Joetzjer, Songbai Hong, Wei Li, et al.. Future Drought-Induced Tree Mortality Risk in Amazon Rainforest. *Earth's Future*, 2024, 12 (8), 10.1029/2023ef003740 . hal-04675023

**HAL Id: hal-04675023**

**<https://hal.science/hal-04675023v1>**

Submitted on 22 Aug 2024

**HAL** is a multi-disciplinary open access archive for the deposit and dissemination of scientific research documents, whether they are published or not. The documents may come from teaching and research institutions in France or abroad, or from public or private research centers.

L'archive ouverte pluridisciplinaire **HAL**, est destinée au dépôt et à la diffusion de documents scientifiques de niveau recherche, publiés ou non, émanant des établissements d'enseignement et de recherche français ou étrangers, des laboratoires publics ou privés.

# Earth's Future

## RESEARCH ARTICLE

10.1029/2023EF003740

# Future Drought-Induced Tree Mortality Risk in Amazon Rainforest



### Key Points:

- We used a land surface model forced by ISIMIP2 climate data to simulate the future drought-induced tree mortality risk in Amazon rainforest
- While climate models differ in projections of wetting/drying patterns, many of them suggest a drying trend in the northeastern Amazon
- Simulations forced by HadGEM model indicate the Guiana Shield and East-central Amazon will transition from carbon sink to source from 2050s

### Supporting Information:

Supporting Information may be found in the online version of this article.

### Correspondence to:

Y. Yao,  
yitong.yao@lsce.ipsl.fr

### Citation:

Yao, Y., Ciaïis, P., Joetzjer, E., Hong, S., Li, W., Zhu, L., & Viovy, N. (2024). Future drought-induced tree mortality risk in Amazon rainforest. *Earth's Future*, 12, e2023EF003740. <https://doi.org/10.1029/2023EF003740>

Received 14 APR 2023

Accepted 29 APR 2024

### Author Contributions:

**Conceptualization:** Yitong Yao, Philippe Ciaïis, Emilie Joetzjer, Nicolas Viovy

**Data curation:** Yitong Yao






**Formal analysis:** Yitong Yao

**Funding acquisition:** Philippe Ciaïis, Nicolas Viovy

**Supervision:** Philippe Ciaïis, Emilie Joetzjer, Nicolas Viovy

**Writing – original draft:** Yitong Yao

**Writing – review & editing:** Yitong Yao, Philippe Ciaïis, Emilie Joetzjer, Songbai Hong, Wei Li, Lei Zhu, Nicolas Viovy

Yitong Yao<sup>1</sup> , Philippe Ciaïis<sup>1</sup> , Emilie Joetzjer<sup>2</sup>, Songbai Hong<sup>3</sup> , Wei Li<sup>4</sup> , Lei Zhu<sup>1,4</sup>, and Nicolas Viovy<sup>1</sup> 

<sup>1</sup>Laboratoire des Sciences du Climat et de l'Environnement, LSCE/IPSL, CEA-CNRS-UVSQ, Université Paris-Saclay, Gif-sur-Yvette, France, <sup>2</sup>INRAE, Université de Lorraine, AgroParisTech, Nancy, France, <sup>3</sup>School of Urban Planning and Design, Shenzhen Graduate School, Peking University, Shenzhen, China, <sup>4</sup>Department of Earth System Science, Ministry of Education Key Laboratory for Earth System Modeling, Institute for Global Change Studies, Tsinghua University, Beijing, China

**Abstract** The future evolution of the Amazon rainforest remains uncertain not only due to uncertain climate projections, but also owing to the intricate balance between tree growth and mortality. Many Earth System Models inadequately represent forest demography processes, especially drought-induced tree mortality. In this study, we used ORCHIDEE-CAN-NHA, a land surface model featuring a mechanistic hydraulic architecture, a tree mortality sub-model linked to a critical loss of stem conductance and a forest demography module for simulating regrowth. The model was forced by bias-corrected climate forcing data from the ISIMIP-2 program, considering two scenarios and four different climate models to project biomass changes in the Amazon rainforest until 2100. These climate models display diverse patterns of climate change across the Amazon region. The simulation conducted with the HadGEM climate model reveals the most significant drying trend, suggesting that the Guiana Shield and East-central Amazon are approaching a tipping point. These two regions are projected to transition from carbon sinks to carbon sources by the mid-21st century, with the Brazilian Shield following suit around 2060. This transition is attributed to heightened drought-induced carbon loss in the future. This study sheds light on uncertainties in the future carbon sink in the Amazon forests, through a well-calibrated model that incorporates tree mortality triggered by hydraulic damage and the subsequent recovery of drought-affected forests through demographic processes.

**Plain Language Summary** Whether the Amazon rainforest will remain as net carbon sink or not has long been of great concern as the drought events are predicted to become more frequent and more intense in the future and such extreme events highly threaten the forest net carbon uptake capacity. Here we use a process-based model embedding drought-induced tree mortality scheme that can perform well regarding past drought events over Amazon basin, to predict the future drought-induced tree mortality risk and the evolution of net biomass carbon sink. The climate models present consistent warming but different wetting/drying patterns, although most of them consistently predict a drier trend in northeastern Amazon. Simulations forced by one climate model showed a carbon sink turning to a carbon source in more than half of Amazon rainforest since the middle of the 21st century. This work can inform the forest area with high tree mortality risk in the future, which calls for more concerns on mitigation policies.

## 1. Introduction

The Amazon rainforest biome is a crucial concern due to its vast yet fragile carbon and biodiversity reserves. Intact Amazon forests hold more than 20% of terrestrial species, house 100 billion tons of carbon (Feldpausch et al., 2012), absorb atmospheric CO<sub>2</sub>, and regulate regional and continental climates by recycling moisture (Werth & Avissar, 2004; Zemp et al., 2017). Despite these critical functions, the stability and spatial continuity of the forest are threatened by climate extreme events such as droughts and storms, widespread deforestation in the South, East, and South-West regions, as well as forest degradation in adjacent areas. These factors increase the risk of reaching a tipping point, where intact forests may transition to carbon sources and even collapse within a few decades. As a result, it is crucial to reduce uncertainties and better understand the likelihood of such a tipping point, and take mitigative actions to preserve the health and resilience of the Amazon rainforest.

Increasing biomass mortality triggered by recent drought events, which seem to be more frequent and severe than in the early 20th century was suggested to explain the decline in net biomass carbon sink during the past three

© 2024. The Author(s).

This is an open access article under the terms of the [Creative Commons Attribution-NonCommercial-NoDerivs License](https://creativecommons.org/licenses/by/4.0/), which permits use and distribution in any medium, provided the original work is properly cited, the use is non-commercial and no modifications or adaptations are made.

decades, despite a continuing but decelerating increase of tree growth rate (Brienen et al., 2015). The carbon sink strength thus weakens in the Amazon intact forests (Phillips & Brienen, 2017). When added to degradation, fires and deforestation losses, the Brazilian Amazon biome, and certainly its South-eastern part, appears to be losing carbon to the atmosphere (Gatti et al., 2021; Qin et al., 2019). Given likely more severe climate condition by the end of the 21st century, for example, with hot and dry clusters in the northeastern Amazon (Vogel et al., 2020) and a longer dry season in the southern and eastern regions (Boisier et al., 2015), it is important to predict the future trajectory of carbon balance in intact rainforests, and anticipate the degree beyond which their structure and function would be highly threatened. Such knowledge is fundamental to provide early warning information, and form policy-relevant strategies to protect this vital biome.

Since the beginning of the 21st century, several severe drought events hit large regions of the intact Amazon rainforest. The 2005 and 2010 drought events and the 2015–2016 extreme El Niño have been evaluated for their impacts on growth and mortality through forest inventory plot data like from the RAINFOR network (Berenguer et al., 2021; Doughty et al., 2015; Feldpausch et al., 2016; Phillips et al., 2009). Besides labor-intensive, scarce, and precious field measurements, satellite data were also used to investigate drought effects. Temporal auto-correlation with long-time series of remote sensing data reflecting ecosystem response has been used to detect early warning signals of reduced resilience or inadequate recovery (Liu et al., 2019; Saatchi et al., 2021). LiDAR-based tree height measurements following the severe drought of 2005 was also used to show post-drought mortality in the epicenter region of that drought (Yang et al., 2018). Decreased resilience to drought was also found over the last 30 years from C-band radar back-scatter time series analysis (Tao et al., 2022). While forest inventory data and satellite products are valuable in assessing past drought effects, they do not provide insights into future projections. The future is likely to bring novel conditions such as elevated CO<sub>2</sub> levels, droughts in regions that have not experienced them before, and emerging nutrient limitations. Thus, it is essential to consider the increasing likelihood of more frequent, warmer, and severe droughts in the 21st century when projecting changes in forest dynamics and their carbon balance (Parsons, 2020). To do so, process-based models that incorporate the key mechanisms of ecosystem-level physiological responses can provide a valuable tool for projecting these changes. By utilizing these models, we can better understand how the Amazon rainforest will respond to future environmental changes and take steps to mitigate the impacts.

Process-based models have been employed to examine the mid-Holocene drought in the Amazon region. This period is of interest due to its drier climate and lower levels of human intervention than the present day. Specifically, these models have investigated aspects of tree cover resilience (Kukla et al., 2021) and the possibility of tree die-back (Smith et al., 2022) during this time period. Smith et al. (2022) focused on mid-Holocene drying as an analog to the drier future, and used model versus paleo-data comparisons to assess the risk of a future Amazon rainforest dieback, based on the higher vulnerability and sensitivity to mid-Holocene drought reconstructed in transitional areas of the southern Amazon. The rainforest in central Amazon remained intact in response to drier climate condition in that study. Nevertheless, we still lack spatially explicit simulations of the Amazon forest dynamics based on tree demography, droughts mortality, recovery after drought, and interactions between climate change and rising CO<sub>2</sub>, which will altogether determine biomass changes in the future. Therefore, a critical need has emerged to predict the response of Amazon rainforest with more realistic process-based models.

Tree mortality from drought constitutes one of the most uncertain processes that affects the simulation of the Amazon biomass carbon stocks sensitivity to climate change, due to knowledge gaps on plant hydraulics (Trugman et al., 2021), large variations of the response across different species, insufficient understanding of the mechanistic linkages between plant stress and tree mortality. This has resulted in multiple empirical mortality parameterizations by modelers therein (Liu, Peng, et al., 2021; Xu et al., 2021). To improve models' performance for reproducing climate-induced tree mortality, the physiological mechanisms underlying tree dieback were encapsulated in models, and evaluated against field evidence. Water demand down-regulation by an insufficient xylem water supply is an indispensable process for modeling plant hydraulic architecture in ecosystem-level or individual-based demography models. Here the Darcy law is used to approximate the plant hydrodynamics, and requires the calculation of water potentials coupled to water supply to upper organs and water demand, and changes in water holding capacitance (Kennedy et al., 2019; Xu et al., 2016). Safety-efficiency trade-off gives a theory to optimize the response of stomatal conductance during drought, although it may not occur as strongly as predicted (Gleason et al., 2016). Tree hydraulic models help to refine the simulation of water flow from soil-root-stem-leaf continuum, water potential and water conductance of each organ, so that hydraulic-failure related loss of tree vitality can be predicted, which is a condition for being able to model mortality due to cavitation. Hence, a

mechanistic hydraulic architecture in a model allows to connect environmental water stress and tree mortality through modeling plant hydrodynamics.

Yet, little is known about how trees die and thus how mortality can be modeled. Different formulations of tree mortality have been attempted including theoretical formulations, empirical or statistical models (related to tree growth), and mechanistic processes from physiological mechanisms (Bugmann et al., 2019). Nonetheless, full plant hydraulics process-based models have rarely been used to predict future mortality risk at regional spatial scales (Trugman, 2021). In this study, we used the recently developed and calibrated process-based model ORCHIDEE-CAN-NHA (Yao, Joetzjer, et al., 2022) with a simplified tree demography module (Joetzjer et al., 2022; Naudts et al., 2015), a mechanistic hydraulic architecture module to simulate plant hydrodynamics from soil to atmosphere, and a mortality module based on the persistence of tree conductance loss and empirical equations to prescribe the size class of trees that are killed. This model was demonstrated to perform well against experimental drought studies at Caxiuanã in eastern Amazon, and Tapajos in east-central Brazilian Amazon (Yao, Joetzjer, et al., 2022). At larger scale for simulations across intact forests of the Amazon, the model was also able to reproduce the decelerating net carbon sink trend over the last three decades, and the field-observed drought sensitivity of trees growth and mortality during recent severe drought events (Yao, Ciais, et al., 2022). In this study, we aim to predict the future biomass carbon sink trajectory and investigate the mortality risk over intact rainforests in the Amazon basin. To account for the uncertainty in future climate, the simulations were performed using outputs of four different climate models. Because climate models have huge biases over the Amazon, especially of precipitation (Ahlström et al., 2017), the climate fields were bias corrected first using the harmonized procedure of the Inter-Sectoral Impact Model Inter-comparison Project (ISIMIP) and further for constraining the interannual variability of future precipitation using historical data (see below). The climate forcing was also downscaled to a spatial resolution of  $0.5^\circ \times 0.5^\circ$  by ISIMIP. The climate models are IPSL-CM5A-LR, GFDL-ESM2M, HadGEM2-ES, and MIROC5. The specific aims of this study are:

1. What are the spatiotemporal features of future droughts projected by climate models, and are those future droughts more severe/frequent than past ones?
2. What is the uncertainty of regional biomass carbon change caused by differences in climate projections?
3. Which part of the Amazon rainforest are consistently most vulnerable or closer to reach a tipping point of switching from a carbon sink to a source?

## 2. Materials and Methods

### 2.1. The Land Surface Model ORCHIDEE-CAN-NHA

In ORCHIDEE-CAN (Naudts et al., 2015), the dynamic vegetation canopy structure is discretized into a user-defined number of circumference classes ( $n = 20$  in this study); then the between-cohorts competition is realized through one empirical self-thinning relationship set in the model and the recruitment rate of young trees is related to leaf area index (LAI). Canopy level GPP is downscaled into the different circumference classes. Background mortality is simulated as the reciprocal of a constant residence time, in addition to self-thinning mortality. ORCHIDEE-CAN-NHA (Yao, Joetzjer, et al., 2022) added a mechanistic hydraulic architecture and a hydraulic-failure induced mortality sub model to ORCHIDEE-CAN. The full name of ORCHIDEE-CAN-NHA is Organizing Carbon and Hydrology in Dynamic Ecosystems—CANopy—New Hydraulic Architecture. In this new version, dynamic  $\frac{1}{2}$  hourly water potentials, water flows along the water potential gradient, and change in water transport conductance and plant organs water storage are simulated. For mortality, the key plant water stress indicator is the percentage loss of stem conductance (PLC), which is assumed to relate to tree mortality through two empirical parameters, a cumulated drought exposure threshold (in days), and a tree mortality fraction in each tree size cohort during each time step when exposure is exceeding the threshold. There is no field measurement for these two parameters, so they were calibrated at the world's longest running through-fall exclusion (TFE) manipulation experiment of Caxiuanã (Rowland et al., 2015) and the model results for biomass mortality were evaluated against data from another TFE site, at Tapajos (Yao, Joetzjer, et al., 2022). Further model validation at regional scale can be found in Text S1 to S3 in Supporting Information S1 including validation of aboveground biomass (AGB), LAI, AGB changes and drought responses.

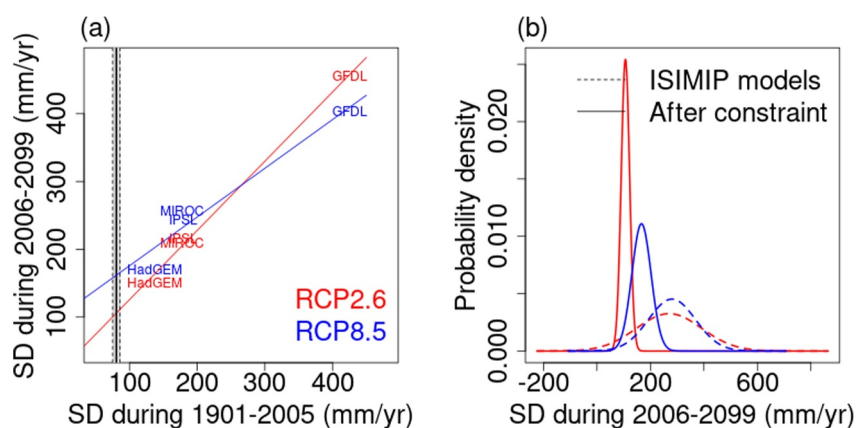


**Figure 1.** Quasi-emergent constraint on the model-simulated Amazon rainfall. (a) Amazon rainfall inter-annual standard deviation (SD) in the past (1901–2005) versus that in the future (2006–2099) among four models. The black vertical dashed line denotes the SD of the past from CRUJRA,  $\sim 80 \text{ mm yr}^{-1}$ . The SD of each ISIMIP model seems to be overestimated compared to that of CRUJRA. (b) PDF for the SD over 2006–2099 in four GCMs. The continuous lines were derived by applying the SD constraint from CRUJRA to the across-model relationship shown in (a). The dashed lines show the Gaussian distribution of original SD assuming that all the ISIMIP models' results are equally correct.

## 2.2. Treatment of ISIMIP (Inter-Sectoral Impact Model Intercomparison Project) Forcing Data

The ISIMIP (Phase 2) project provides an ensemble of downscaled, bias corrected climate forcing based on different models and RCP scenarios. Four global climate models (GCMs) from ISIMIP, (GFDL-ESM2M, HadGEM-2ES, IPSL-CM5A-LR, MIROC5) and two emission scenarios (RCP2.6, RCP8.5) contribute to eight gridded climate fields for the future. These climate forcing are used to force ORCHIDEE-CAN-NHA. Four GCMs from CMIP5 (Coupled Model Intercomparison Project Phase 5) were selected as in Frieler et al., 2017. Since bias in precipitation is huge and influences the modeled mean aboveground biomass, with climate models showing a large dry bias without bias correction (Ahlström et al., 2017), the ISIMIP forcing procedure, in addition to downscaling the climate forcing to  $0.5^\circ$  also uses a bias correction (Hempel et al., 2013). Namely, spatial and seasonal patterns of climate variables were corrected upon the Climatic Research Unit (CRU) fields for the period 1960–1990. This bias correction removes the mean and seasonal precipitation bias, but the inter-annual variability of climate models remains as originally simulated by GCMs during the historical period and the future. This means that ISIMIP models may have either too many or too severe droughts, or the opposite, during the current period, and this bias can persist in the future. Correction for the mean value of climate variables could be sufficient to evaluate the mean productivity but not for investigating tree mortality that depends on extreme events. Therefore, we used an emergent constraint method (Cox et al., 2013) to resample the future inter-annual variability so that the present-day variability of each climate model is realistic when compared to observations from CRUJRA2.1 (Harris, 2019), where the correction also allows to keep the change in climate variability in the future.

We found that the climate models have a larger than observed inter-annual standard deviation (SD) of rainfall over the historical period and a larger standard deviation in the future as well (Figure 1). All models over-estimate the observed SD. Therefore, we designed a quasi-emergent constraint method by constraining the future expected SD based on the relationship between present and future across the models, as shown in Figure 1. The constraint is the observed SD from CRUJRA2.1 over 1901–2005. We first calculate annual rainfall over Amazon basin (basin map in Figure S1 in Supporting Information S1). We then do a bias correction of the mean value and SD of rainfall over the historical and future periods. For calibrating SD, we define an initial threshold of  $M \pm x \times \text{SD}$  at the basin level, where  $M$  is the mean rainfall value of each ISIMIP model,  $\text{SD}$  is the inter-annual standard deviation of each model, and  $x$  is a parameter adjusted for four ISIMIP models individually. If the annual precipitation in a given year is above the upper bound (or below the lower bound) defined by  $M \pm x \times \text{SD}$ , the annual precipitation is set to be equal to the upper (or lower) limit. This correction is performed iteratively on basin-level annual precipitation until the corrected SD is closer to the constrained one, so that the expected SD is constrained as shown in Figure 1. Then a correction ratio was derived as the “corrected” annual precipitation dividing the “uncorrected” one, which can be applied to the whole basin. As the mean value of precipitation in GCMs is still tens of millimeter away from the reanalysis data, we refer to the multiplicative method used in Hempel et al. (2013), by applying a ratio

**Table 1**  
*Description of Simulations Performed in This Study*

	Climate forcing	Atmospheric CO <sub>2</sub>	Mortality module	Restart point	
Spin-up stage 1	1861–1880	Constant (286 ppm)	Deactivated	/	/
Spin-up stage 2	1861–1880	Constant (286 ppm)	Activated	Stage1	/
S—historical	1861–2005	Increasing	Activated	Stage2	Historical
S—future	2006–2099	Increasing	Activated	End of S - historical	RCP 2.6 RCP 8.5
S—future— constant CO <sub>2</sub>	2006–2099	Constant (378.8 ppm)	Activated	End of S - historical	RCP 8.5

*Note.* Due to the limitation of computation resources, S-future-constant CO<sub>2</sub> simulation was carried out only for RCP8.5 scenario.

derived from the mean annual rainfall from the baseline one (CRUJRA) divided by that from four ISIMIP forcing on top of the precipitation data. In total, the precipitation forcing data was corrected by two ratio values, one for SD, and one for the mean value. This corrected precipitation forcing was used in our model simulation. The change in mean annual precipitation after our another-round bias correction is shown in Table S1 in Supporting Information S1.

### 2.3. Simulation Protocol

To initialize carbon pools from the ORCHIDEE-CAN-NHA model simulations, we designed a two-step spin-up. During the first spin-up, the model recycles the climate forcing data of the period 1861–1880 with constant CO<sub>2</sub> concentration of 286 ppm and a constant mortality, which reflects longevity-inversed metric and also self-thinning parameterizations of the model. At the end of this first spin-up stage, biomass carbon storage reaches an equilibrium. Then, a second spin-up takes the end of the first one as starting point. During the second spin-up stage, the model recycles the climate forcing data during 1861–1880 with constant CO<sub>2</sub> concentration of 286 ppm but its mortality scheme is activated. The drought events during 1861–1880 then lead the model to reach another dynamic equilibrium, with less biomass, as caused by recurrent drought mortality. After the second spin up, the historical and future simulations followed the protocols shown in Table 1.

### 2.4. Drought Severity (Climatological Water Deficit)

Following previous research on the evaluation of drought area and severity (Papastefanou et al., 2022), the maximum cumulative water deficit (MCWD) was used to compare droughts, as given by Equations 1 and 2. A fixed value for evapotranspiration (ET) of ~100 mm per month is used (Phillips et al., 2009). When monthly rainfall is below 100 mm, the forest undergoes water deficit. The water deficit accumulates over the hydrological year from October in the previous year to September in the current one. MCWD is the most negative value of the cumulative water deficit among all 12 months. Then decadal mean of MCWD over the whole period was subtracted from the MCWD of a year with drought, giving a MCWD anomaly.

$$CWD_m = CWD_{m-1} + P_m - 100 \text{ if } P_m < 100, \text{ else } CWD_m = 0 \quad (1)$$

with m being the month 1, ...12 (1 = October)

$$MCWD = \min(CWD_m), m = 1, \dots, 12 \quad (2)$$

### 2.5. Diagnostic of Aboveground Biomass Dynamics

From the model outputs, the net annual aboveground biomass change ( $\Delta$ AGB), AGB gain and loss are calculated over each hydrological year. The AGB “gross” gain is the carbon allocated to the growth of aboveground sapwood in cohorts with DBH above 10 cm, each year. Note that the model includes a conversion of sapwood to heartwood which does not changes the net growth. The AGB “gross” loss is the biomass mortality of aboveground sapwood and heartwood in cohorts with DBH above 10 cm, each year.  $\Delta$ AGB is the difference between AGB

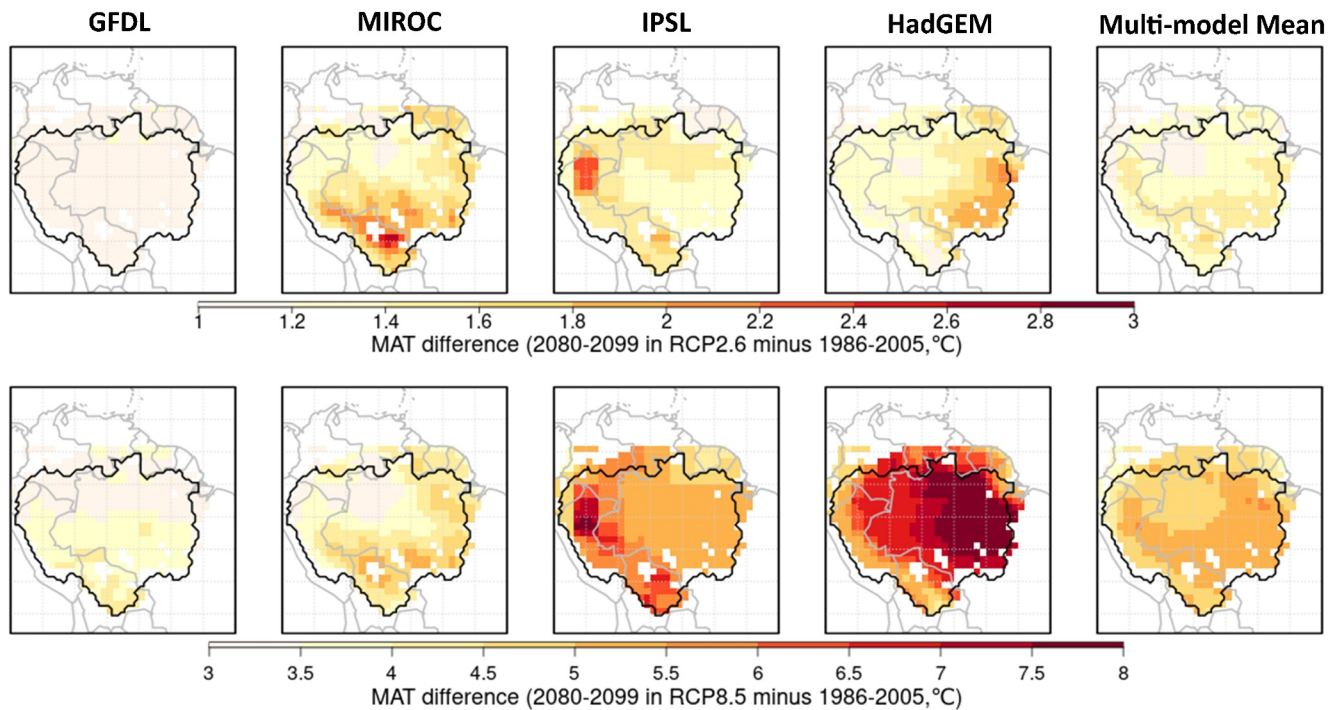


**Figure 2.** Evolution of future temperature change shown as the difference between MAT (mean annual temperature) during the last 20 years by the end of the 21st century (2080–2099) and MAT during 1986–2005. Top panels: RCP2.6, bottom panels: RCP8.5.

gain and AGB loss. The anomaly during a drought year  $k$  is derived by subtracting the average value ( $\mu$ ) over the whole period by Equations 3–5. The recruitment also constitutes a part of growth, however, here to be comparable with the inventories that only sample trees individuals with DBH above 10 cm, the growth of saplings less than 10 cm in diameter is not included in the diagnostic of model output.

$$\Delta \text{AGB}_{\text{anomaly}} = \Delta \text{AGB}_k - \mu_{\Delta \text{AGB}} \quad (3)$$

$$\text{AGB}_{\text{gain}}_{\text{anomaly}} = \text{AGB}_{\text{gain}}_k - \mu_{\text{AGB}_{\text{gain}}} \quad (4)$$

$$\text{AGB}_{\text{loss}}_{\text{anomaly}} = \text{AGB}_{\text{loss}}_k - \mu_{\text{AGB}_{\text{loss}}} \quad (5)$$

Linear regression was performed between carbon fluxes and MCWD anomalies relative to multi-year mean values to obtain the net carbon change sensitivity.

## 2.6. Model Evaluation Statistics

We used the R programming environment and statistical packages (version 3.5.0; R Core Team, 2019) for all data processing and analysis. Package “ncdf4 v1.17” (Pierce, 2019) is used to handle files in NetCDF format from model outputs. Package “fields v10.3” (Nychka et al., 2020) is used in AGB change and climate metrics mapping.

## 3. Results

### 3.1. Quantification of Future Climate Evolution

Warming is widespread across the whole Amazon basin by the end of this century in all GCMs, yet with heterogeneous pattern and different hotspots (Figure 2). In the RCP2.6 scenario, IPSL and MIROC show a warming of higher magnitude than other climate models, especially in southern Amazon for MIROC and western Amazon for IPSL. The mean warming across models is of  $1.3 \pm 0.3^\circ\text{C}$  in 2080–2099 compared to the period 1986–2005. The geographic extent of the warming trend expands and intensifies in the RCP8.5 scenario, with an average warming of  $4.9 \pm 1.4^\circ\text{C}$ . As shown in Figure 2, two models (GFDL and MIROC) show a lower warming

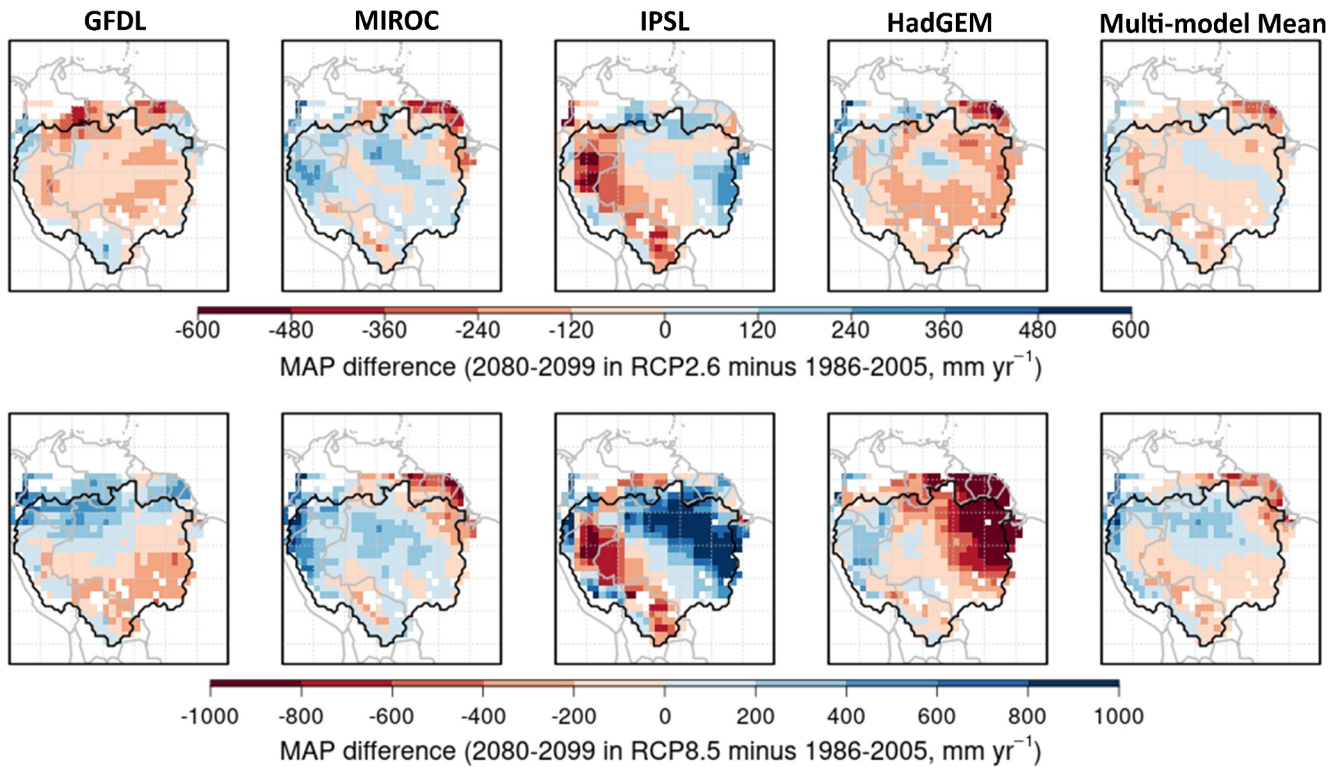


**Figure 3.** Same as Figure 2 but for mean annual precipitation (MAP) changes.

especially in the southern Amazon (less than 5°C), while one model (HadGEM) shows the largest warming, mainly in the eastern Amazon (about 7°C).

The vapor pressure deficit (VPD) is a critical factor driving evaporative demand, and thus of the water stress on plants in our model. In our model, a higher VPD increases the transpiration demand which initially acts to increase transpiration but can reduce it later when soil moisture is limiting. A higher VPD reduces stomatal conductance and photosynthesis in the model formulation (Yin & Struik, 2009). Figure S2 in Supporting Information S1 shows the change of VPD between the end of this century (2080–2099) and the recent historical period (1986–2005). Similar to the pattern of temperature change, in both RCP2.6 and RCP8.5 scenarios, the IPSL climate model predicts a VPD increase in western Amazon. The MIROC climate model predicts a VPD increase in southern Amazon and eastern Amazon. The HadGEM climate model predicts greater VPD increase in eastern Amazon. VPD increase estimated by GFDL forcing is less obvious than that in other models in both RCP2.6 and RCP8.5 scenarios (Figure S2 in Supporting Information S1). Globally VPD largely follows the pattern of temperature change (Figure 2 and Figure S2 in Supporting Information S1).

With regard to rainfall changes, the climate models simulate drying and wetting trends across different sub-regions of the Amazon basin as shown in Figure 3. There is less agreement among the four climate models than for temperature and VPD changes. In the RCP2.6 scenario, MIROC and HadGEM show a wetting trend in the western Amazon and a drying trend in the northeastern Amazon, more extensive in HadGEM. The IPSL model shows a wetting trend from the central Amazon to the east side, but the GFDL model shows extensive drying trend over this area. The wetting-drying dipole is similar between RCP2.6 and RCP8.5 scenario in each climate model, but more contrasted in the RCP8.5 scenario, with a rainfall difference between dipoles reaching as much as 1,000 mm yr<sup>-1</sup> (note the different color scales for each scenario in Figure 3). The climate models' predictions exhibit little agreement on the area with greater drying trend. The most consistent pattern is that drought events in northeastern Amazon occur more frequently in all the models, associated with higher temperature, higher VPD and a decline of precipitation.

The MCWD shows a drying trend spatially consistent with the pattern of precipitation reductions, as shown in Figure 4. MCWD reflects the accumulation of water deficit especially in the dry season with monthly rainfall



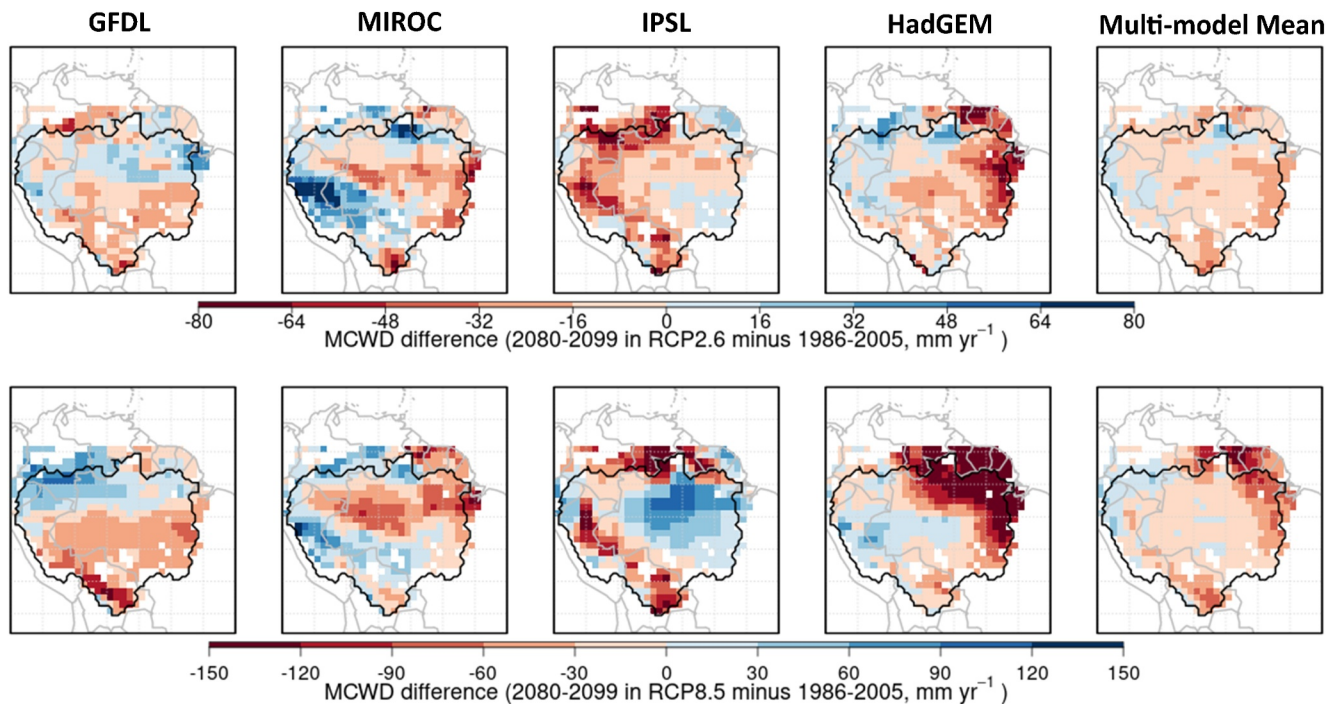


**Figure 4.** Same as Figure 2 but for maximum cumulative water deficit (MCWD) changes.

below 100 mm (see Section 2.4). The MIROC climate model is the only one that shows different pattern between MAP and MCWD change, as the increase of MCWD difference reveals greater water stress in central and eastern Amazon (Figure 4). Three models, GFDL, IPSL and HadGEM, present similar patterns of MCWD and temperature changes, with more water stress in southern Amazon in the GFDL climate model, a drier trend in western Amazon detected in the IPSL climate model, and more severe water stress in the northeastern Amazon in HadGEM (Figure 2).

### 3.2. Change of the Biomass Carbon Sink

Figure 5 presents the distribution of  $\Delta$ AGB, the biomass carbon sink, during 20-yr periods in the historical Era and the future, with the area experiencing different magnitude of  $\Delta$ AGB. By the end of the 21st century in the RCP2.6 scenario, the area where the forest is a net carbon source (from biomass only) is a bit more extensive in the IPSL simulation than the area being a carbon sink. For the net Amazon biomass carbon balance, growth continues to exceed mortality in the period 2080–2099 (source:  $-0.12 \text{ PgC yr}^{-1}$  vs. sink:  $0.17 \text{ PgC yr}^{-1}$ ). In comparison, the area being a carbon source is smaller than the one of sink in GFDL, MIROC, and HadGEM. These results account for the effect of  $\text{CO}_2$  driving a larger  $\text{CO}_2$  uptake when it increases. Atmospheric  $\text{CO}_2$  peaks at 442.8 ppm by 2052 in RCP2.6 and then declines slightly to 421 ppm by 2100, which drives a small decline in photosynthesis uptake after the peak, in absence of climate change. In the IPSL and HadGEM models for the RCP2.6 scenario, regional sinks slightly exceed sources, and the Amazon intact forests remains a net carbon sink, with a magnitude comparable to the historical period with the HadGEM model ( $0.04 \text{ PgC yr}^{-1}$  in the past vs.  $0.02 \text{ PgC yr}^{-1}$  in the future) and the magnitude shrinking with the IPSL model ( $0.15 \text{ PgC yr}^{-1}$  in the past vs.  $0.04 \text{ PgC yr}^{-1}$  in the future). In the GFDL climate model, the Amazon rainforest turns to be a small net carbon source in the RCP2.6 scenario ( $-0.02 \text{ PgC yr}^{-1}$ ). In the MIROC model, we found a small net carbon sink in the future, but a carbon source in the historical period due to a huge drought estimated by the MIROC model for year 2005, even with our SD bias correction (Figure S3 in Supporting Information S1). This drought event is stochastic in the MIROC model and the modeled carbon balance differs from RAINFOR forest plot observations upscaled to the entire Amazon.

In the RCP8.5 scenario, regional carbon sinks and sources intensify, following the patterns of wetting and drying regions respectively. The HadGEM forcing leads us to simulate a net carbon source across the whole Amazon of  $0.5 \text{ PgC yr}^{-1}$ , which is composed of a  $0.57 \text{ PgC yr}^{-1}$  carbon source mainly located in the northeastern Amazon

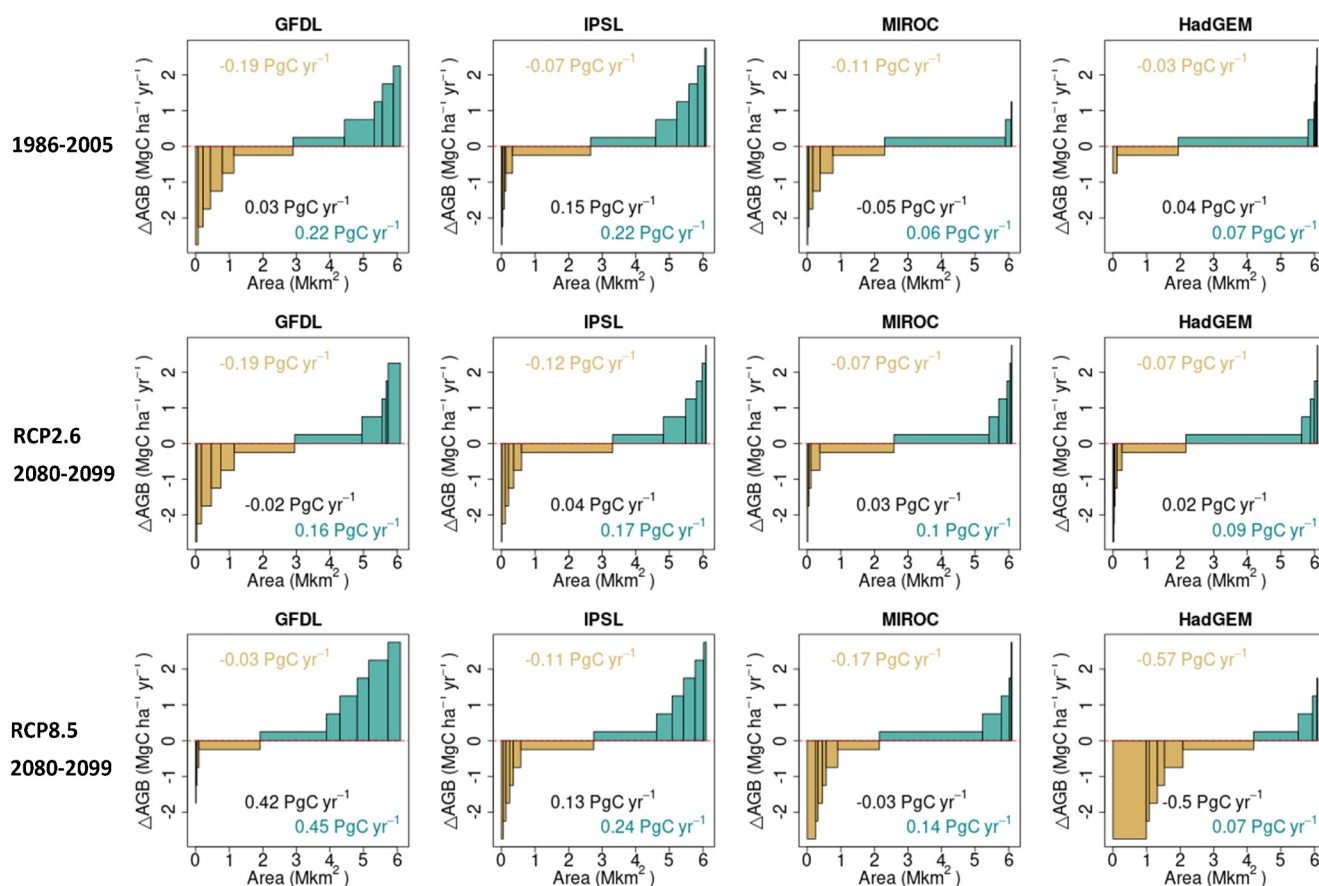


**Figure 5.** Net biomass carbon fluxes densities during 2080–2099 for two climate scenarios, and 1986–2005 (y-axis) and the area (x-axis) for different intensity categories, presented in decreasing order of net carbon sink densities. Total carbon budget is labeled in the panel, separated by carbon source (dark-yellow color) and carbon sink (cyan).

where extreme warming occurs (Figure 2), outweighing a 0.07 PgC yr<sup>-1</sup> carbon sink in other regions (Figure 5). MIROC also leads to a small net carbon source of 0.03 PgC yr<sup>-1</sup>. In contrast, the simulations forced by GFDL and IPSL all predict a higher carbon sink relative to the historical period (GFDL: 0.45 vs. 0.22 PgC yr<sup>-1</sup>, IPSL: 0.24 vs. 0.22 PgC yr<sup>-1</sup>). The carbon source driven by GFDL shrinks in the future (−0.19 vs. −0.03 PgC yr<sup>-1</sup>) whereas the magnitude of net carbon loss increases in IPSL simulation (−0.07 vs. −0.11 PgC yr<sup>-1</sup>). Our simulation results all include the positive effect on forest growth of rising CO<sub>2</sub> by 479.3 ppm between the present period and 2080–2099 in RCP8.5.

Besides the differences of mean carbon balance estimate between two time periods, we also found that there is a large inter-annual variation of net biomass change during the historical period and in the future (Figure S4 in Supporting Information S1). By the end of the 21st century, years with positive and negative net biomass change appear in the RCP2.6 scenario. The frequency distribution of carbon sources and sinks in the last 20 years of the historical period and in the future simulation is shown in Figure 6. In the RCP2.6 scenario, the number of years with a source does not increase relative to the historical period. In the RCP8.5 scenario, however, the number of years with a source increases, and the magnitude of carbon source anomalies also increases in Guiana Shield, East-central Amazon and Brazilian Shield in the HadGEM simulations. In the RCP8.5 scenario, the results forced by HadGEM show that the Guiana Shield and East-Central Amazon turn to become net carbon sources after around 2045. The Brazilian Shield also becomes a carbon source in this model after around 2060 (Figure S4 in Supporting Information S1). We only found a “tipping-point” from sink to source over the whole Amazon in the simulation forced by the HadGEM climate data (Figure S4 in Supporting Information S1). Through a comparison between model simulations with and without drought-induced tree mortality scheme, we demonstrate that such sink-source transition is attributed to heightened drought-induced carbon loss (Figure S5 in Supporting

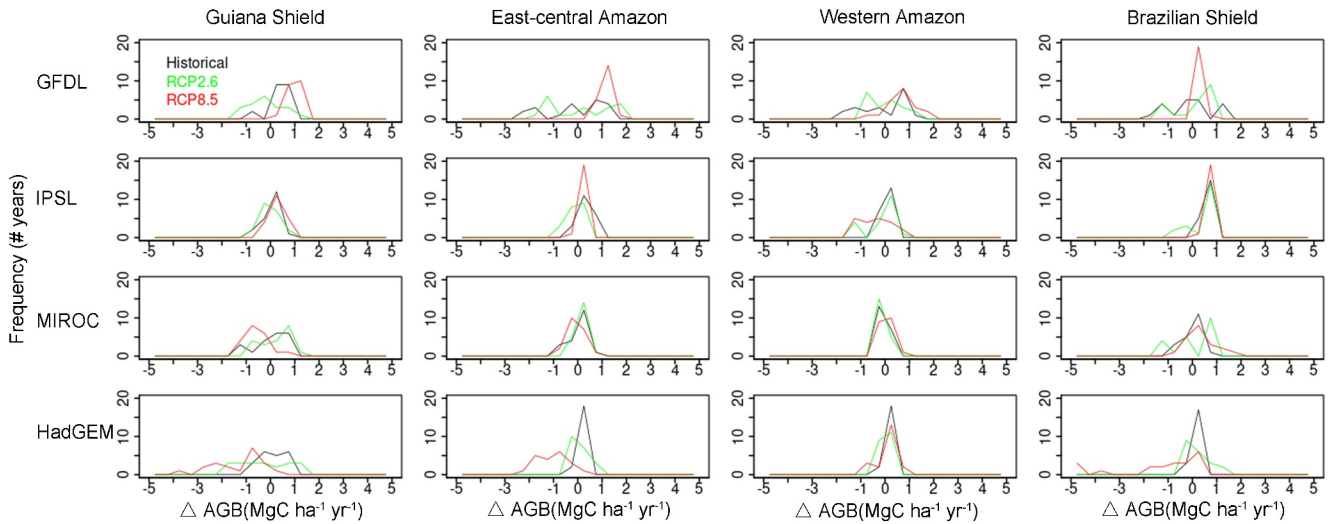


**Figure 6.** The frequency distribution of carbon source years and carbon sink years. The comparison is made between the last 20 years of the historical period (1986–2005) and the future (2080–2099).

Information S1). The drought-induced tree mortality results in an additional carbon loss of  $0.56 \text{ PgC yr}^{-1}$  over the Amazon basin ( $0.57$  vs.  $0.01 \text{ PgC yr}^{-1}$ , Figure S6 in Supporting Information S1).

We also analyzed model agreement on the prediction of net biomass change. Figure 7 shows that in the RCP2.6 scenario, simulations forced by the four climate models agree on the sign of net biomass change in Brazilian Shield but diverge in the Guiana Shield. In the RCP8.5 scenario, three simulations agree on a weaker biomass carbon sink in western Amazon and Brazilian Shield but disagree on the sign of the carbon balance in the Guiana Shield and East-central Amazon.

### 3.3. Comparison of Drought Sensitivity Between the Past and the Future

For the future, given the large divergence of regional rainfall change prediction among the four climate models, we still lack agreement on the occurrence of possible extreme events if we use the Z score transformed MCWD as metrics to investigate changes of  $\Delta\text{AGB}$  to MCWD. Figure 8 shows the anomalies in  $\Delta\text{AGB}$  corresponding to the anomalies in mean annual temperature (MAT) and MCWD. It can be seen clearly that less water deficit (positive MCWD anomaly) and cooler condition (negative MAT anomaly) correspond to positive  $\Delta\text{AGB}$

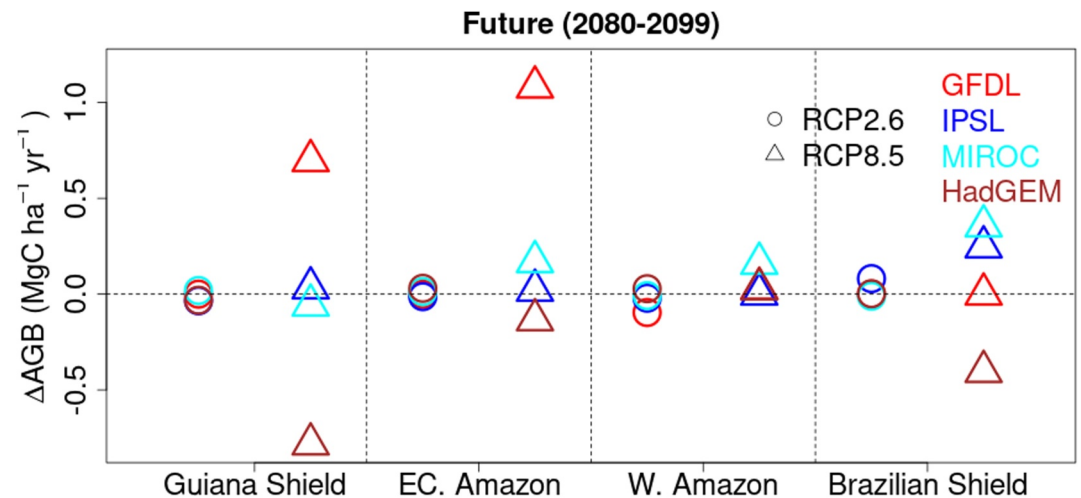


**Figure 7.**  $\Delta\text{AGB}$  during the future (2080–2099). Circle: RCP2.6, triangle: RCP8.5. The color of these symbols represents the simulations driven by different climate models.

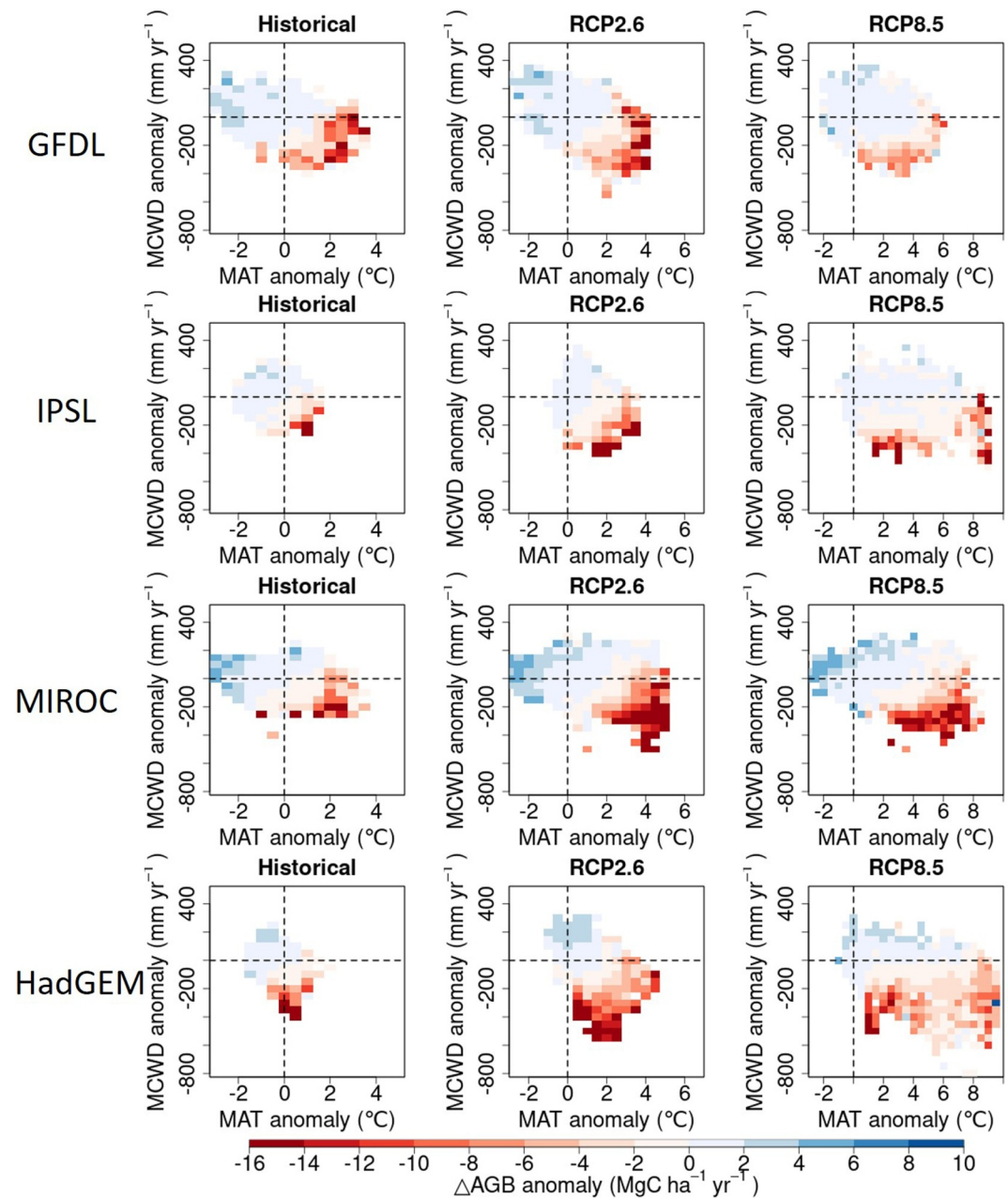


**Figure 8.** Composite maps showing  $\Delta\text{AGB}$  annual anomaly in each year (Historical: 1986–2005, Future: 2006–2099) corresponding to MCWD anomalies and MAT anomalies calculated with a baseline period set to 1986–2005. Negative MCWD anomaly denotes years with more severe water stress. Positive MAT anomaly denotes warmer years. Blue box means a positive  $\Delta\text{AGB}$  anomaly relative to the whole period, and a red box the negative  $\Delta\text{AGB}$  anomaly. The temperature and water deficit anomalies were binned to different intervals and the  $\Delta\text{AGB}_{\text{anomaly}}$  in each interval was calculated.

anomalies or more biomass carbon accumulation, as expected. For example, the simulation forced by the MIROC climate model shows that the  $\Delta\text{AGB}$  anomaly can be  $+4 \text{ MgC ha}^{-1} \text{ yr}^{-1}$  in a year when the annual temperature is  $2^\circ\text{C}$  lower and MCWD is 200 mm higher than the baseline period. When temperature anomalies turn out to be positive and water deficit anomalies are negative, negative  $\Delta\text{AGB}$  anomalies appear in the bottom-right corner of each panel, corresponding to dry extremes. As shown in Figure 8, an interesting finding is that the sensitivity of  $\Delta\text{AGB}$  anomaly is not symmetrical between wet and dry extreme events no matter which period is considered (historical or future). Warmer-drier events correspond to more AGB loss than the AGB increase under colder-wetter events of same absolute magnitude. For example, simulations forced by the MIROC and HadGEM

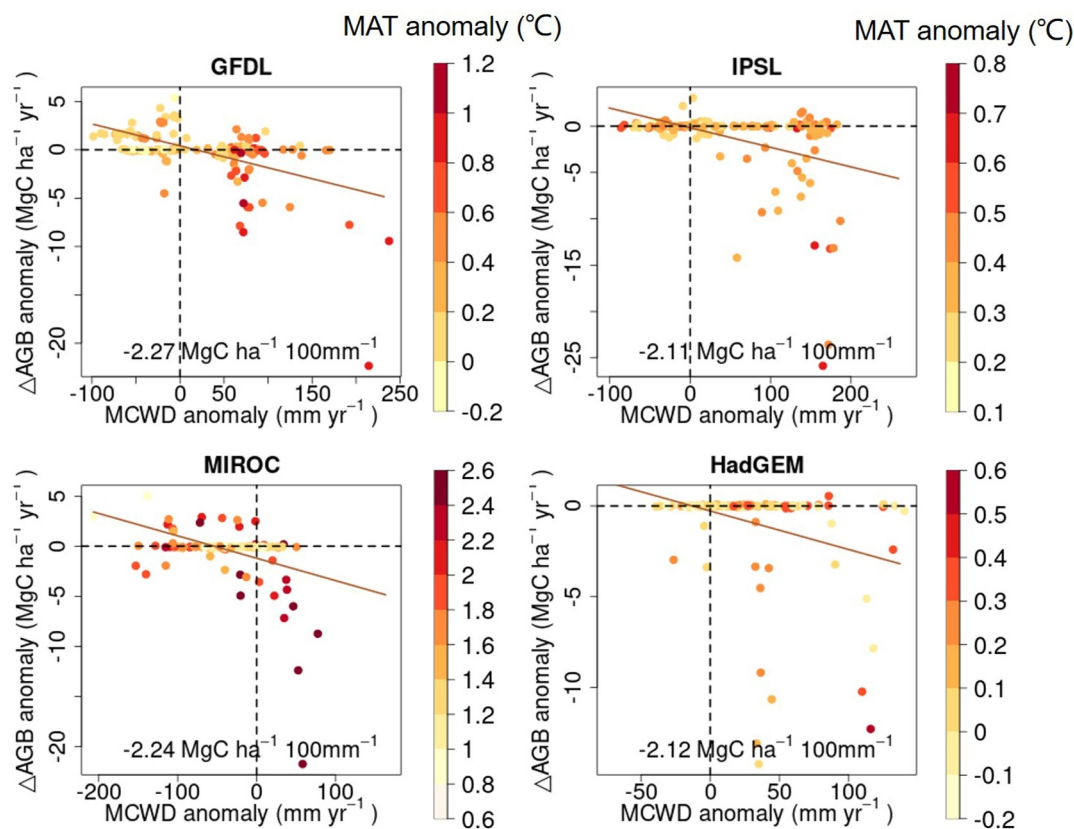


**Figure 9.** Net biomass change versus drought severity in western Amazon. Severity is defined from MCWD, with higher positive values denoting more acute water stress. The color of the points corresponds to mean annual temperature anomaly, with darker color meaning warmer condition. The continuous lines denote the best model fit. Here, to be comparable with the plot in Phillips et al. (2009), positive MCWD anomaly means more severe water stress as an exception.

climate models showed higher magnitudes of net biomass loss (more than  $-6 \text{ MgC ha}^{-1} \text{ yr}^{-1}$ ) than the magnitudes of net carbon accumulation (less than  $+6 \text{ MgC ha}^{-1} \text{ yr}^{-1}$ ) given similar but opposite variations in MAT and MCWD. It should be noted that the biomass loss due to tree mortality risk is also related to the background AGB, therefore the  $\Delta\text{AGB}$  anomaly is not always more negative under RCP8.5 scenario due to its less accumulated biomass.

## 4. Discussion

### 4.1. Drought Risk

Future climate change over the Amazon shows a large uncertainty as evidenced by the spread among the four climate models we used from ISIMIP2b (Frierler et al., 2017). There seems to be however some agreement between these models and the larger CMIP5 ensemble on an average rainfall decrease in the Amazon basin in the future (Chen et al., 2014). In the four models used, a warmer and drier tendency diagnosed from the air temperature and water deficit variables prevails in the future. This translates into a higher drought-induced tree mortality risk over the Amazon intact rainforest. To the best of our knowledge, this study is one of the first that predicts future changes in the Amazon rainforest biomass and tree dieback in response to drought with a process-based model incorporating a mechanistic hydraulic architecture coupled to a tree mortality model, whose results compared well with forest inventory data for two recent droughts (Yao, Ciais, et al., 2022). Without plant hydraulics related mortality, many process-based models did not reproduce the observed biomass loss and decrease of individual density with regard to observed field data at drought manipulation experiments (Powell et al., 2013).

Our model simulation forced by the ISIMIP historical forcing captured the negative relationship between net biomass change anomalies and MCWD anomalies, as shown in Figure 9. The drought sensitivity simulated by the

CRUJRA forcing is about  $2.0 \text{ MgC ha}^{-1}$  of net carbon loss per 100 mm increase in MCWD (Yao, Ciaia, et al., 2022). Here, the four climate models showed droughts in the epicenter of western Amazon in different years since droughts from ISIMIP models are stochastic and not synchronized with the real world. Model-derived drought sensitivity in the epicenter of the western Amazon ranged from  $-2.11$  to  $-2.27 \text{ MgC ha}^{-1}$  per 100 mm increase in MCWD, broadly comparable with the forest inventory plot analysis from Phillips et al. (2009) of  $-2.5 \text{ MgC ha}^{-1}$  per 100 mm, also with more contribution from increased carbon loss than from decreased growth, like in the observations.

When forced by the HadGEM climate, we predict a higher tree mortality and correspondingly a greater biomass loss in northeastern and eastern Amazon, especially in the RCP8.5 scenario. This simulation indicates a transition from a carbon sink to a carbon source in the Guiana Shield and East-central Amazon by the middle of the 21st century, highlighting the potential vulnerability of these regions. This finding is not surprising since the eastern part of the Amazon tends to experience more significant dry-season water stress (Duffy et al., 2015; Malhi et al., 2009), a faster warming trend, and a greater water deficit as reflected by MCWD. Several studies have examined the future evolution of the Amazon basin's carbon balance. An earlier study by Poulter et al. (2010) used LPJml forced by 8 GCMs and found that both HadCM3 and HadGEM (IPCC-AR4 models) predicted large biomass loss over most Amazon basin by the end of the 21st century, when competition-induced biomass carbon loss was considered. Huntingford et al. (2013) using the MOSES-TRIFFID land surface scheme forced by 22 climate models (CMIP3), predicted that Amazon intact rainforest carbon sinks will prevail with climate change, where only one climate model (HadCM3) predicted the biomass loss till the end of the 21st century although this land surface model did not account for drought-induced tree mortality process. A more recent study by Shi et al. (2021) combined 5 process-based models and 4 climate projections from ISIMIP2b, and found that high-emission scenarios predict a carbon sink saturation at the end of 21st century whereas low-emission pathway would induce decline in carbon sink strength over almost whole Amazon basin since the middle of this century, where only one land surface model (improved LPJml) considered tree mortality depending on climate stress, tree density and growth vigor whereas other models simply resorted to constant values like the inverse of turnover or tree longevity as background mortality rate. The climate projections, their corresponding emission pathway and model structure all contribute to the uncertainty underlying the predictions of carbon sink strength evolution in Amazon rainforest. In addition to these process-based models, Hubau et al. (2020) employed a linear mixed model incorporating environmental variables of  $\text{CO}_2$ , MAT and MCWD to predict the future tropical forest carbon sink. Using interpolated temperature increase gradients derived from both observational records and CMIP5, their statistical model forecasts a much lower carbon sink compared to recent observations, with the net carbon sink approaching zero by around 2040. This warning signal emerges slightly ahead of our process-based model predictions, possibly attributed to the discrepancy between the pronounced inter-annual climate forcing variations used in our process-based models and the smoother climate trends derived from interpolated data used in their statistical models.

Our prediction of biomass loss in northeastern Amazon with a model resolving hydraulic failure and mortality deserves attention since the maximum tree height therein is the highest (Gorgens et al., 2021) and taller trees importantly affect the local ecosystem functioning given their dominance in global carbon budget (Gora & Esquivel-Muelbert, 2021). Our simulation forced by the HadGEM climate model shows a higher tree mortality rate in cohorts with DBH higher than 40 cm at the end of this century (Figure S7 in Supporting Information S1), consistent with those field data found during manipulated drought (Rowland et al., 2015). The sensitivity of carbon dynamics related to tree height still has not reached consensus. On the one hand, the photosynthesis of tall trees in Amazonia was found to be less sensitive to rainfall inter-annual variability than the shorter trees using solar-induced fluorescence data, the mechanism proposed being that deeper root system of taller trees give them access to ground water (Giardina et al., 2018). On the other hand, the narrower hydraulic safety margin of taller trees suggests that they are more vulnerable to drought-induced water stress (Liu, Chen, et al., 2021). From the drought manipulation experiment at Caxiuanã site, taller trees were found to have less negative  $\Psi_{50}$  and died first (Rowland et al., 2015). Therefore, the availability of deep soil water source and also the possible shift of intrinsic hydraulic characteristics co-determine the response of tall trees to future drought risks. Further efforts on analyzing the RAINFOR data to see if taller trees also die first during these mega droughts are required to fill the knowledge gap in identifying the relative importance of these two factors in shaping taller trees performance.

In this study, we found that a warmer-drier trend appears in most of the Amazon basin although its intensity and geographic span vary among the four ISIMIP2b climate model projections and emission pathways. Since our

model (ORCHIDEE-CAN-NHA) was calibrated against a drought experiment with only exclusion of rainfall, our “calibrated” sensitivity to rain-out condition may be an underestimation relative to the reality since the field data did not consider the combined effects of higher temperature and VPD with soil moisture deficits. Compound precipitation deficits and aridity events are largely co-occurring (Zhou et al., 2019), in which mortality thresholds could be more rapidly reached than by soil water stress alone. The indirect effect of drought on stomatal closure was found to outweigh the direct negative biochemical response to high temperature as deduced from an experimental drought study (Smith et al., 2020), which suggests that several degrees of temperature increase may still be tolerated by trees before photosynthesis limitation occurs. Huntingford et al. (2013) used sensitivity simulations by perturbing only one factor of temperature, rainfall and atmospheric CO<sub>2</sub> to demonstrate that the predictions of the change in forest carbon across Amazon by the end of the 21st century were more sensitive to variation in temperature and atmospheric CO<sub>2</sub> concentration than to alteration in rainfall. Shi et al. (2021) found a more negative sensitivity of carbon sink strength to temperature increase under higher CO<sub>2</sub> levels in the Amazon basin except the southwestern region but less distinct effect on precipitation sensitivity through factorial simulations. Besides the CO<sub>2</sub> fertilization effect on photosynthesis included in models, Yao, Ciais, et al. (2022) confirmed an alleviation of drought risk under current CO<sub>2</sub> concentration (in the historical period) through a decline in the number of days with exposure to a mortality risk. Here through a simulation with constant CO<sub>2</sub> concentration fixed to 2005 level (Table 1), where the biomass carbon stocks would be lower than the scenario of elevated CO<sub>2</sub> as we found in similar setup in Yao, Ciais, et al. (2022), we found an increase of tree mortality risk in the absence of CO<sub>2</sub> effects over almost half area of Amazon basin, but it is the reduction of biomass growth without CO<sub>2</sub> fertilization effect that dominates the more negative carbon balance rather than the more elevated tree mortality risk (in absence of soil moisture deficit being partly alleviated by elevated CO<sub>2</sub>). Studies manipulating seedlings have shown that elevated levels of CO<sub>2</sub> did not alter the time required for plants to reach a water stress threshold during drought conditions (Gattmann et al., 2021). Additionally, nutrient limitations such as phosphorus may hinder the growth response to elevated CO<sub>2</sub> levels. However, these limitations can also result in reduced water consumption during the wet season, benefiting productivity in the dry season to some extent (Goll et al., 2018). Therefore, it remains to be seen whether the stress alleviation of tree dieback resulting from elevated CO<sub>2</sub> levels will persist over the long term. This could be tested through ongoing observation treatments, such as the Amazon FACE experiment.

The tree mortality risk is modulated by soil texture, where sandy soil tends to show greater resilience and resistance than that of clay soil (Longo et al., 2018). Yet, in reality soil texture also affects the nutrient availability, drainage state, and thus the biomass growth rates. For example, sand-rich soil performs poor in retaining nutrients, but such soil can be naturally selected for slow-growing trees that may invest more carbon into preservation of hydraulic safety (Oliveira et al., 2019). With regard to the anticipation of the future drought sensitivity, plant water use strategies determined by hydraulic traits and soil texture should be included in models for improving the knowledge of forest response since soil hydraulics can also determine the degree of isohydricity (Javaux & Carminati, 2021).

#### 4.2. Asymmetry of Net Biomass Change Between Wet and Dry Conditions

A difference in sensitivity between wet and dry conditions was found in our simulations, as evidenced by the net biomass change in wet extremes versus dry extremes as shown in Figure 8. Such nonlinear relationship between net biomass changes and climate anomalies implies that carbon loss induced by a drought year is hardly compensated by gains from wet extremes, namely, a negative asymmetry. It should be noticed that the possible negative effects from wet events of unexpected flood can trigger carbon source as well, which has not been included in the model. Theoretically both dry and wet extremes impose negative effects on tree growth and mortality rate can thus be elevated in both cases. However, the sequential occurrence of wet and dry extremes can buffer their respective adverse effects, which is modulated by the water table depth or namely local soil hydrologic condition (Esteban et al., 2021). Drought events lead to tree dieback and recovery may be slowed down due to incomplete recovery in hydraulic transport system or nonstructural carbohydrate reserves. Conversely, wet years without disturbances can contribute to more growth without a positive legacy effect. The forest's nonlinear response to precipitation anomalies can be influenced by various factors, including the duration of events (Felton et al., 2021) and nutrient limitations (Goll et al., 2018). The debate over whether legacy effects or compensatory effects have a more significant impact on the forest's response remains unresolved and calls for further evidence

from field measurements or satellite detection. The results of such research can then be incorporated into process-based models to benefit our understanding of the forest's complex response to changing environmental conditions.

### 4.3. Limit of the Current Approach and Perspective for Improving Projections

#### 4.3.1. Legacy Effects After Drought

Legacy mortality effects from drought are not captured by Earth System Models (Anderegg et al., 2015), although satellite products confirmed their existence in the Amazon, like a decline in carbon sink several years after the drought (Tao et al., 2022; Yang et al., 2018, 2022). Accumulative metrics or variables with a memory effect should be analyzed to understand legacy tree growth in model simulation. Besides, acclimation to warmer or drier condition should be also considered as another aspect of legacy. Ignoring the adaptation mechanism would underestimate the ecosystem resilience (Singh et al., 2022), which is the characteristic with the lowest recovery pace after disturbance (Poorter et al., 2021).

#### 4.3.2. Hydraulic Traits

Uncertainty of the modeled drought-induced mortality risk also arises from our setup of constant hydraulic traits for one plant functional type describing all intact rainforests. In other words, in our model, plant water regulation does not have spatial or temporal variation. Both intra- and inter-species variation of hydraulic traits exist and temporal shift of trait also occurs depending on surrounding hydric condition. The Caxiuanã study found that resistant species had more negative  $\Psi_{50}$  value and were less vulnerable to the water stress (Rowland et al., 2015). The growth of hydraulic-stressed trees was more affected by their hydraulic traits rather than by their allocation-related traits (Rowland et al., 2021). Variation of hydraulic traits is also linked to ecosystem community composition (Lourenço Junior et al., 2022). Therefore, more comprehensive plant trait data could be assimilated into a model like ORCHIDEE-CAN-NHA to define a more realistic hydraulic response, for example, starting with isohydric or anisohydric characteristics.

We acknowledge that the uncertainties associated with future climate signals and in the sensitivity of forest response both affect the spread of biomass change projections. Including new processes in process-based models like drought-induced tree mortality, which are very sensitive to extreme events, increases the uncertainties in vegetation model response to climate change. Huntingford et al. (2013) found that it is the physiological processes of DGVMs, or namely the implicitly-formulated sensitivity, rather than uncertainties among climate projections, that dominated the uncertainties in future carbon storage trajectory. To further clarify the impact of drought on Amazon intact forests, more collaboration between experimentalists and modelers remains necessary, with ground-based truth of field campaigns, and inventories data collected during and after droughts. Considering the projected increase in the intensity and frequency of drought events in the 21st century and possible concurring tree mortality, strategies should be developed and implemented to manage risks and improve the ecosystem adaption capacity.

## 5. Conclusion

A process-based model incorporating plant hydraulics, self-thinning mortality, and drought-induced tree mortality, ORCHIDEE-CAN-NHA, was forced by historical climate reconstruction and bias-corrected future climate forcing from ISIMIP-2 program to predict the future biomass carbon dynamics and tree mortality risk over the Amazon rainforest. The future climate evolution in Amazon shows a widespread warming trend, although its magnitude varies among climate models. A pronounced increase in the maximum cumulative water deficit (MCWD) is also found, but different regional patterns emerge from the four climate models. The only consistent pattern observed across various climate models for MCWD is a drier trend in the northeastern Amazon region. Among the models, the simulation forced by the HadGEM climate model in the RCP8.5 scenario showed the most pronounced drying in the eastern and northeastern Amazon regions, indicating a tipping point where the carbon sinks in the Guiana Shield and East-central Amazon could turn into carbon sources by the middle of the 21st century. Such transition from sink to source also appears in Brazilian Shield after around 2060. This study makes an important step forward by providing a spatial image of the likelihood of drought risks and predicting the evolution of future Amazon rainforest net carbon balance, by resorting to a well-calibrated model that incorporates hydraulic failure induced tree mortality, and subsequent recovery from demographic processes,



including recruitment and growth of survivor trees. The predicted possible vulnerability state of Amazon rainforest required further investigation and concerns on mitigation policies.

### Conflict of Interest

The authors declare no conflicts of interest relevant to this study.

### Data Availability Statement

The model simulation outputs are available in Yao (2023).

### Acknowledgments

This work was financially supported by the CLAND Convergence Institute funded by ANR (16-CONV-0003). YY also acknowledges support from Make Our Planet Great Again (MOPGA) Scholarship. This work was performed using HPC/AI resources from GENCI-TGCC (Grant 6328).

### References

- Ahlström, A., Canadell, J. G., Schurgers, G., Wu, M., Berry, J. A., Guan, K., & Jackson, R. B. (2017). Hydrologic resilience and Amazon productivity. *Nature Communications*, 8, 1–9. <https://doi.org/10.1038/s41467-017-00306-z>
- Anderegg, W. R., Schwalm, C., Biondi, F., Camarero, J. J., Koch, G., Litvak, M., et al. (2015). Pervasive drought legacies in forest ecosystems and their implications for carbon cycle models. *Science*, 349(6247), 528–532. <https://doi.org/10.1126/science.aab1833>
- Berenguer, E., Lennox, G. D., Ferreira, J., Malhi, Y., Aragão, L. E., Barreto, J. R., et al. (2021). Tracking the impacts of El Niño drought and fire in human-modified Amazonian forests. *Proceedings of the National Academy of Sciences of the United States of America*, 118(30), e2019377118. <https://doi.org/10.1073/pnas.2019377118>
- Boisier, J. P., Ciais, P., Ducharne, A., & Guimberteau, M. (2015). Projected strengthening of Amazonian dry season by constrained climate model simulations. *Nature Climate Change*, 5(7), 656–660. <https://doi.org/10.1038/nclimate2658>
- Brienen, R. J., Phillips, O. L., Feldpausch, T. R., Gloor, E., Baker, T. R., Lloyd, J., et al. (2015). Long-term decline of the Amazon carbon sink. *Nature*, 519(7543), 344–348. <https://doi.org/10.1038/nature14283>
- Bugmann, H., Seidl, R., Hartig, F., Bohn, F., Brūna, J., Cailleret, M., et al. (2019). Tree mortality submodels drive simulated long-term forest dynamics: Assessing 15 models from the stand to global scale. *Ecosphere*, 10(2), e02616. <https://doi.org/10.1002/ecs2.2616>
- Chen, H., Sun, J., & Chen, X. (2014). Projection and uncertainty analysis of global precipitation-related extremes using CMIP5 models. *International Journal of Climatology*, 34(8), 2730–2748. <https://doi.org/10.1002/joc.3871>
- Cox, P. M., Pearson, D., Booth, B. B., Friedlingstein, P., Huntingford, C., Jones, C. D., & Luke, C. M. (2013). Sensitivity of tropical carbon to climate change constrained by carbon dioxide variability. *Nature*, 494(7437), 341–344. <https://doi.org/10.1038/nature11882>
- Doughty, C. E., Metcalfe, D., Girardin, C., Amezquita, F. F., Cabrera, D. G., Huasco, W. H., et al. (2015). Drought impact on forest carbon dynamics and fluxes in Amazonia. *Nature*, 519(7541), 78–82. <https://doi.org/10.1038/nature14213>
- Duffy, P. B., Brando, P., Asner, G. P., & Field, C. B. (2015). Projections of future meteorological drought and wet periods in the Amazon. *Proceedings of the National Academy of Sciences of the United States of America*, 112(43), 13172–13177. <https://doi.org/10.1073/pnas.1421010112>
- Esteban, E. J., Castilho, C. V., Melgaço, K. L., & Costa, F. R. (2021). The other side of droughts: Wet extremes and topography as buffers of negative drought effects in an Amazonian forest. *New Phytologist*, 229(4), 1995–2006. <https://doi.org/10.1111/nph.17005>
- Feldpausch, T., Phillips, O., Brienen, R., Gloor, E., Lloyd, J., Lopez-Gonzalez, G., et al. (2016). Amazon forest response to repeated droughts. *Global Biogeochemical Cycles*, 30(7), 964–982. <https://doi.org/10.1002/2015gb005133>
- Feldpausch, T. R., Lloyd, J., Lewis, S. L., Brienen, R. J., Gloor, M., Monteagudo Mendoza, A., et al. (2012). Tree height integrated into pantropical forest biomass estimates. *Biogeosciences*, 9(8), 3381–3403. <https://doi.org/10.5194/bg-9-3381-2012>
- Felton, A. J., Knapp, A. K., & Smith, M. D. (2021). Precipitation–productivity relationships and the duration of precipitation anomalies: An underappreciated dimension of climate change. *Global Change Biology*, 27(6), 1127–1140. <https://doi.org/10.1111/gcb.15480>
- Frieler, K., Lange, S., Piontek, F., Reyer, C. P., Schewe, J., Warszawski, L., et al. (2017). Assessing the impacts of 1.5 C global warming–simulation protocol of the Inter-Sectoral Impact Model Intercomparison Project (ISI-MIP2b). *Geoscientific Model Development*, 10(12), 4321–4345. <https://doi.org/10.5194/gmd-10-4321-2017>
- Gatti, L. V., Basso, L. S., Miller, J. B., Gloor, M., Domingues, L. G., Cassol, H. L., et al. (2021). Amazonia as a carbon source linked to deforestation and climate change. *Nature*, 595(7867), 388–393. <https://doi.org/10.1038/s41586-021-03629-6>
- Gattmann, M., Birami, B., Nadal Sala, D., & Ruehr, N. K. (2021). Dying by drying: Timing of physiological stress thresholds related to tree death is not significantly altered by highly elevated CO<sub>2</sub>. *Plant, Cell and Environment*, 44(2), 356–370. <https://doi.org/10.1111/pce.13937>
- Giardina, F., Konings, A. G., Kennedy, D., Alemohammad, S. H., Oliveira, R. S., Uriarte, M., & Gentine, P. (2018). Tall Amazonian forests are less sensitive to precipitation variability. *Nature Geoscience*, 11(6), 405–409. <https://doi.org/10.1038/s41561-018-0133-5>
- Gleason, S. M., Westoby, M., Jansen, S., Choat, B., Hacke, U. G., Pratt, R. B., et al. (2016). Weak tradeoff between xylem safety and xylem-specific hydraulic efficiency across the world's woody plant species. *New Phytologist*, 209(1), 123–136. <https://doi.org/10.1111/nph.13646>
- Goll, D. S., Joetzier, E., Huang, M., & Ciais, P. (2018). Low phosphorus availability decreases susceptibility of tropical primary productivity to droughts. *Geophysical Research Letters*, 45(16), 8231–8240. <https://doi.org/10.1029/2018gl077736>
- Gora, E. M., & Esquivel-Muelbert, A. (2021). Implications of size-dependent tree mortality for tropical forest carbon dynamics. *Nature Plants*, 1–8.
- Gorgens, E. B., Nunes, M. H., Jackson, T., Coomes, D., Keller, M., Reis, C. R., et al. (2021). Resource availability and disturbance shape maximum tree height across the Amazon. *Global Change Biology*, 27(1), 177–189. <https://doi.org/10.1111/gcb.15423>
- Harris, I. C. (2019). CRU JRA: Collection of CRU JRA forcing datasets of gridded land surface blend of Climatic Research Unit (CRU) and Japanese reanalysis (JRA) data. *Centre for Environmental Data Analysis*. <http://catalogue.ceda.ac.uk/uuid/863a47a6d8414b6982e1396c69a9efe8>
- Hempel, S., Frieler, K., Warszawski, L., Schewe, J., & Piontek, F. (2013). A trend-preserving bias correction—the ISI-MIP approach. *Earth System Dynamics*, 4(2), 219–236. <https://doi.org/10.5194/esd-4-219-2013>
- Hubau, W., Lewis, S. L., Phillips, O. L., Affum-Baffoe, K., Beeckman, H., Cuní-Sánchez, A., et al. (2020). Asynchronous carbon sink saturation in African and Amazonian tropical forests. *Nature*, 579(7797), 80–87. <https://doi.org/10.1038/s41586-020-2035-0>
- Huntingford, C., Zelazowski, P., Galbraith, D., Mercado, L. M., Sitch, S., Fisher, R., et al. (2013). Simulated resilience of tropical rainforests to CO<sub>2</sub>-induced climate change. *Nature Geoscience*, 6(4), 268–273. <https://doi.org/10.1038/ngeo1741>

- Javaux, M., & Carminati, A. (2021). Soil hydraulics affect the degree of isohydricity. *Plant Physiology*, *186*(3), 1378–1381. <https://doi.org/10.1093/plphys/kiab154>
- Joetzer, E., Maignan, F., Chave, J., Goll, D., Poulter, B., Barichivich, J., et al. (2022). Effect of tree demography and flexible root water uptake for modeling the carbon and water cycles of Amazonia. *Ecological Modelling*, *469*, 109969. <https://doi.org/10.1016/j.ecolmodel.2022.109969>
- Kennedy, D., Swenson, S., Oleson, K. W., Lawrence, D. M., Fisher, R., Lola da Costa, A. C., & Gentile, P. (2019). Implementing plant hydraulics in the community land model, version 5. *Journal of Advances in Modeling Earth Systems*, *11*(2), 485–513. <https://doi.org/10.1029/2018ms001500>
- Kukla, T., Ahlström, A., Maezumi, S. Y., Chevalier, M., Lu, Z., Winnick, M. J., & Chamberlain, C. P. (2021). The resilience of Amazon tree cover to past and present drying. *Global and Planetary Change*, *202*, 103520. <https://doi.org/10.1016/j.gloplacha.2021.103520>
- Liu, L., Chen, X., Ciais, P., Yuan, W., Maignan, F., Wu, J., et al. (2021). Tropical tall forests are more sensitive and vulnerable to drought than short forests. *Global Change Biology*, *28*(4), 1583–1595. <https://doi.org/10.1111/gcb.16017>
- Liu, Q., Peng, C., Schneider, R., Cyr, D., Liu, Z., Zhou, X., & Kneeshaw, D. (2021). TRIPLEX-Mortality model for simulating drought-induced tree mortality in boreal forests: Model development and evaluation. *Ecological Modelling*, *455*, 109652. <https://doi.org/10.1016/j.ecolmodel.2021.109652>
- Liu, Y., Kumar, M., Katul, G. G., & Porporato, A. (2019). Reduced resilience as an early warning signal of forest mortality. *Nature Climate Change*, *9*(11), 880–885. <https://doi.org/10.1038/s41558-019-0583-9>
- Longo, M., Knox, R. G., Levine, N. M., Alves, L. F., Bonal, D., Camargo, P. B., et al. (2018). Ecosystem heterogeneity and diversity mitigate Amazon forest resilience to frequent extreme droughts. *New Phytologist*, *219*(3), 914–931. <https://doi.org/10.1111/nph.15185>
- Lourenço Junior, J., Enquist, B. J., von Arx, G., Sonsin-Oliveira, J., Morino, K., Thomaz, L. D., & Milanez, C. R. D. (2022). Hydraulic tradeoffs underlie local variation in tropical forest functional diversity and sensitivity to drought. *New Phytologist*, *234*(1), 50–63. <https://doi.org/10.1111/nph.17944>
- Malhi, Y., Aragão, L. E., Galbraith, D., Huntingford, C., Fisher, R., Zelazowski, P., et al. (2009). Exploring the likelihood and mechanism of a climate-change-induced dieback of the Amazon rainforest. *Proceedings of the National Academy of Sciences of the United States of America*, *106*(49), 20610–20615. <https://doi.org/10.1073/pnas.0804619106>
- Naudts, K., Ryder, J., McGrath, M. J., Otto, J., Chen, Y., Valade, A., et al. (2015). A vertically discretised canopy description for ORCHIDEE (SVN r2290) and the modifications to the energy, water and carbon fluxes. *Geoscientific Model Development*, *8*(7), 2035–2065. <https://doi.org/10.5194/gmd-8-2035-2015>
- Nychka D, F. R., Paige, J., Sain, S., Gerber, F., & Iverson, M. (2020). *Fields: Tools for spatial data R package version 10.3*. University Corporation for Atmospheric Research. <https://doi.org/10.5065/D6W957CT>
- Oliveira, R. S., Costa, F. R., van Baalen, E., de Jonge, A., Bittencourt, P. R., Almanza, Y., et al. (2019). Embolism resistance drives the distribution of Amazonian rainforest tree species along hydro-topographic gradients. *New Phytologist*, *221*(3), 1457–1465. <https://doi.org/10.1111/nph.15463>
- Papastefanou, P., Zang, C. S., Angelov, Z., de Castro, A. A., Jimenez, J. C., De Rezende, L. F. C., et al. (2022). Recent extreme drought events in the Amazon rainforest: Assessment of different precipitation and evapotranspiration datasets and drought indicators. *Biogeosciences*, *19*(16), 3843–3861. <https://doi.org/10.5194/bg-19-3843-2022>
- Parsons, L. (2020). Implications of CMIP6 projected drying trends for 21st century Amazonian drought risk. *Earth's Future*, *8*(10), e2020EF001608. <https://doi.org/10.1029/2020ef001608>
- Phillips, O. L., Aragão, L. E., Lewis, S. L., Fisher, J. B., Lloyd, J., López-González, G., et al. (2009). Drought sensitivity of the Amazon rainforest. *Science*, *323*(5919), 1344–1347. <https://doi.org/10.1126/science.1164033>
- Phillips, O. L., & Brienen, R. J. (2017). Carbon uptake by mature Amazon forests has mitigated Amazon nations' carbon emissions. *Carbon Balance and Management*, *12*, 1–9. <https://doi.org/10.1186/s13021-016-0069-2>
- Pierce, D. (2019). Package NCDF4. In L. Poorter, D. Craven, C. C. Jakovac, M. T. vander Sande, L. Amissah, F. Bongers, et al. (Eds.), *Multidimensional tropical forest recovery*, *Science* (Vol. 374, pp. 1370–1376). Retrieved from <http://cirrus.ucsd.edu/~pierce/ncdf>
- Poulter, B., Hattermann, F., Hawkins, E., Zaehle, S., Sitch, S., Restrepo-Coupe, N., et al. (2010). Robust dynamics of Amazon dieback to climate change with perturbed ecosystem model parameters. *Global Change Biology*, *16*(9), 2476–2495. <https://doi.org/10.1111/j.1365-2486.2009.02157.x>
- Poorter, L., Craven, D., Jakovac, C. C., van der Sande, M. T., Amissah, L., Bongers, F., et al. (2021). Multidimensional tropical forest recovery. *Science*, *374*, 1370–1376. <https://doi.org/10.1126/science.abh3629>
- Powell, T. L., Galbraith, D. R., Christoffersen, B. O., Harper, A., Imbuzeiro, H. M., Rowland, L., et al. (2013). Confronting model predictions of carbon fluxes with measurements of Amazon forests subjected to experimental drought. *New Phytologist*, *200*(2), 350–365. <https://doi.org/10.1111/nph.12390>
- Qin, Y., Xiao, X., Dong, J., Zhang, Y., Wu, X., Shimabukuro, Y., et al. (2019). Improved estimates of forest cover and loss in the Brazilian Amazon in 2000–2017. *Nature Sustainability*, *2*(8), 764–772. <https://doi.org/10.1038/s41893-019-0336-9>
- R Core Team. (2019). *R: A language and environment for statistical computing*. R Foundation for Statistical Computing. Retrieved from <https://www.R-project.org/>
- Rowland, L., da Costa, A. C. L., Galbraith, D. R., Oliveira, R., Binks, O. J., Oliveira, A., et al. (2015). Death from drought in tropical forests is triggered by hydraulics not carbon starvation. *Nature*, *528*(7580), 119–122. <https://doi.org/10.1038/nature15539>
- Rowland, L., Oliveira, R. S., Bittencourt, P. R., Giles, A. L., Coughlin, I., Costa, P. d.B., et al. (2021). Plant traits controlling growth change in response to a drier climate. *New Phytologist*, *229*(3), 1363–1374. <https://doi.org/10.1111/nph.16972>
- Saatchi, S., Longo, M., Xu, L., Yang, Y., Abe, H., Andre, M., et al. (2021). Detecting vulnerability of humid tropical forests to multiple stressors. *One Earth*, *4*(7), 988–1003. <https://doi.org/10.1016/j.oneear.2021.06.002>
- Shi, H., Tian, H., Pan, N., Reyer, C. P., Ciais, P., Chang, J., et al. (2021). Saturation of global terrestrial carbon sink under a high warming scenario. *Global Biogeochemical Cycles*, *35*(10), e2020GB006800. <https://doi.org/10.1029/2020gb006800>
- Singh, C., van der Ent, R., Wang-Erlandsson, L., & Fetzer, I. (2022). Hydroclimatic adaptation critical to the resilience of tropical forests. *Global Change Biology*, *28*(9), 2930–2939. <https://doi.org/10.1111/gcb.16115>
- Smith, M. N., Taylor, T. C., van Haren, J., Rosolem, R., Restrepo-Coupe, N., Adams, J., et al. (2020). Empirical evidence for resilience of tropical forest photosynthesis in a warmer world. *Nature Plants*, *6*(10), 1225–1230. <https://doi.org/10.1038/s41477-020-00780-2>
- Smith, R. J., Singarayer, J. S., & Mayle, F. E. (2022). Response of Amazonian forests to mid-Holocene drought: A model-data comparison. *Global Change Biology*, *28*(1), 201–226. <https://doi.org/10.1111/gcb.15929>
- Tao, S., Chave, J., Frison, P. L., Le Toan, T., Ciais, P., Fang, J., et al. (2022). Increasing and widespread vulnerability of intact tropical rainforests to repeated droughts. *Proceedings of the National Academy of Sciences of the United States of America*, *119*(37), e2116626119. <https://doi.org/10.1073/pnas.2116626119>

- Trugman, A. T. (2021). Integrating plant physiology and community ecology across scales through trait-based models to predict drought mortality. *New Phytologist*, 234(1), 21–27. <https://doi.org/10.1111/nph.17821>
- Trugman, A. T., Anderegg, L. D., Anderegg, W. R., Das, A. J., & Stephenson, N. L. (2021). Why is tree drought mortality so hard to predict? *Trends in Ecology & Evolution*, 36(6), 520–532. <https://doi.org/10.1016/j.tree.2021.02.001>
- Vogel, M. M., Hauser, M., & Seneviratne, S. I. (2020). Projected changes in hot, dry and wet extreme events' clusters in CMIP6 multi-model ensemble. *Environmental Research Letters*, 15(9), 094021. <https://doi.org/10.1088/1748-9326/ab90a7>
- Werth, D., & Avissar, R. (2004). The regional evapotranspiration of the Amazon. *Journal of Hydrometeorology*, 5(1), 100–109. [https://doi.org/10.1175/1525-7541\(2004\)005<0100:treata>2.0.co;2](https://doi.org/10.1175/1525-7541(2004)005<0100:treata>2.0.co;2)
- Xu, X., Konings, A. G., Longo, M., Feldman, A., Xu, L., Saatchi, S., et al. (2021). Leaf surface water, not plant water stress, drives diurnal variation in tropical forest canopy water content. *New Phytologist*, 231(1), 122–136. <https://doi.org/10.1111/nph.17254>
- Xu, X., Medvigy, D., Powers, J. S., Becknell, J. M., & Guan, K. (2016). Diversity in plant hydraulic traits explains seasonal and inter-annual variations of vegetation dynamics in seasonally dry tropical forests. *New Phytologist*, 212(1), 80–95. <https://doi.org/10.1111/nph.14009>
- Yang, H., Ciais, P., Wigneron, J. P., Chave, J., Cartus, O., Chen, X., et al. (2022). Climatic and biotic factors influencing regional declines and recovery of tropical forest biomass from the 2015/16 El Niño. *Proceedings of the National Academy of Sciences of the United States of America*, 119(26), e2101388119. <https://doi.org/10.1073/pnas.2101388119>
- Yang, Y., Saatchi, S. S., Xu, L., Yu, Y., Choi, S., Phillips, N., et al. (2018). Post-drought decline of the Amazon carbon sink. *Nature Communications*, 9, 1–9. <https://doi.org/10.1038/s41467-018-05668-6>
- Yao, Y. (2023). Model outputs for 'Future drought-induced tree mortality risk in Amazon rainforest' [Dataset]. *Zenodo*. <https://doi.org/10.5281/zenodo.7601015>
- Yao, Y., Ciais, P., Viovy, N., Joetzer, E., & Chave, J. (2022). How drought events during the last Century have impacted biomass carbon in Amazonian rainforests. *Global Change Biology*, 29(3), 747–762. <https://doi.org/10.1111/gcb.16504>
- Yao, Y., Joetzer, E., Ciais, P., Viovy, N., Cresto Aleina, F., Chave, J., et al. (2022). Forest fluxes and mortality response to drought: Model description (ORCHIDEE-CAN-NHA r7236) and evaluation at the Caxiuana drought experiment. *Geoscientific Model Development*, 15(20), 7809–7833. <https://doi.org/10.5194/gmd-15-7809-2022>
- Yin, X., & Struik, P. C. (2009). C3 and C4 photosynthesis models: An overview from the perspective of crop modelling. *NJAS - Wageningen Journal of Life Sciences*, 57(1), 27–38. <https://doi.org/10.1016/j.njas.2009.07.001>
- Zemp, D. C., Schleussner, C.-F., Barbosa, H. M., Hirota, M., Montade, V., Sampaio, G., et al. (2017). Self-amplified Amazon forest loss due to vegetation-atmosphere feedbacks. *Nature Communications*, 8, 1–10. <https://doi.org/10.1038/ncomms14681>
- Zhou, S., Williams, A. P., Berg, A. M., Cook, B. I., Zhang, Y., Hagemann, S., et al. (2019). Land-atmosphere feedbacks exacerbate concurrent soil drought and atmospheric aridity. *Proceedings of the National Academy of Sciences of the United States of America*, 116(38), 18848–18853. <https://doi.org/10.1073/pnas.1904955116>

## References From the Supporting Information

- Avitabile, V., Herold, M., Heuvelink, G. B., Lewis, S. L., Phillips, O. L., Asner, G. P., et al. (2016). An integrated pan-tropical biomass map using multiple reference datasets. *Global Change Biology*, 22(4), 1406–1420. <https://doi.org/10.1111/gcb.13139>
- Cao, S., Li, M., Zhu, Z., Wang, Z., Zha, J., Zhao, W., et al. (2023). Spatiotemporally consistent global dataset of the GIMMS leaf area index (GIMMS LAI4g) from 1982 to 2020. *Earth System Science Data*, 15(11), 4877–4899. <https://doi.org/10.5194/essd-15-4877-2023>
- Feldpausch, T. R., Phillips, O. L., Brienen, R. J. W., Gloor, E., Lloyd, J., Lopez-Gonzalez, G., et al. (2016). Amazon forest response to repeated droughts. *Global Biogeochemical Cycles*, 30(7), 964–982. <https://doi.org/10.1002/2015gb005133>
- Feldpausch, T. R., Banin, L., Phillips, O. L., Baker, T. R., Lewis, S. L., Quesada, C. A., et al. (2011). Height-diameter allometry of tropical forest trees. *Biogeosciences*, 8(5), 1081–1106. <https://doi.org/10.5194/bg-8-1081-2011>
- Hunka, N., Santoro, M., Armston, J., Dubayah, R., McRoberts, R. E., Næsset, E., et al. (2023). On the NASA GEDI and ESA CCI biomass maps: Aligning for uptake in the UNFCCC global stocktake. *Environmental Research Letters*, 18(12), 124042. <https://doi.org/10.1088/1748-9326/ad0b60>
- Hansen, M. C., Potapov, P. V., Moore, R., Hancher, M., Turubanova, S. A., Tyukavina, A., et al. (2013). High-resolution global maps of 21st-century forest cover change. *Science*, 342(6160), 850–853. <https://doi.org/10.1126/science.1244693>
- Johnson, M. O., Galbraith, D., Gloor, E., De Deurwaerder, H., Guimberteau, M., Rammig, A., et al. (2016). Plot data from: "Variation in stem mortality rates determines patterns of aboveground biomass in Amazonian forests: Implications for dynamic global vegetation models" [Dataset]. *ForestPlots.NET*. [https://doi.org/10.5521/FORESTPLOTS.NET/2016\\_2](https://doi.org/10.5521/FORESTPLOTS.NET/2016_2)
- Phillips, O. L., Aragão, L. E., Lewis, S. L., Fisher, J. B., Lloyd, J., López-González, G., et al. (2009). Drought sensitivity of the Amazon rainforest. *Science*, 323(5919), 1344–1347. <https://doi.org/10.1126/science.1164033>
- Xu, L., Saatchi, S. S., Yang, Y., Yu, Y., Pongratz, J., Bloom, A. A., et al. (2021). Changes in global terrestrial live biomass over the 21st century. *Science Advances*, 7(27), eabe9829. <https://doi.org/10.1126/sciadv.abe9829>